
Theranostic GPA33-Pretargeted Radioimmunotherapy of Human Colorectal Carcinoma with a Bivalent ^{177}Lu -Labeled Radiohaptent

Brett A. Vaughn^{1,2}, Sang-gyu Lee³, Daniela Burnes Vargas¹, Shin Seo², Sara S. Rinne^{1,4}, Hong Xu⁴, Hong-fen Guo⁴, Alexandre B. Le Roux^{2,3}, Leah Gajecki³, Simone Krebs^{3,5}, Guangbin Yang⁶, Ouathek Ouerfelli⁶, Pat B. Zanzonico⁷, Edward K. Fung⁸, Samantha St. Jean⁹, Sebastian E. Carrasco⁹, Achim Jungbluth¹⁰, Nai Kong V. Cheung⁴, Steven M. Larson^{2,3}, Darren R. Veach^{3,5}, and Sarah M. Cheal^{1,2}

¹Molecular Imaging Innovations Institute, Department of Radiology, Weill Cornell Medicine, New York, New York; ²Molecular Pharmacology Program, Memorial Sloan Kettering Cancer Center, New York, New York; ³Department of Radiology, Memorial Sloan Kettering Cancer Center, New York, New York; ⁴Department of Pediatrics, Memorial Sloan Kettering Cancer Center, New York, New York; ⁵Department of Radiology, Weill Cornell Medicine, New York, New York; ⁶Organic Synthesis Core Facility, Memorial Sloan Kettering Cancer Center, New York, New York; ⁷Department of Medical Physics, Memorial Sloan Kettering Cancer Center, New York, New York; ⁸Department of Medical Physics, Weill Cornell Medicine, New York, New York; ⁹Laboratory of Comparative Pathology, Memorial Sloan Kettering Cancer Center–Weill Cornell Medicine–Rockefeller University, New York, New York; and ¹⁰Department of Pathology, Memorial Sloan Kettering Cancer Center, New York, New York

Radiolabeled small-molecule DOTA-haptens can be combined with antitumor/anti-DOTA bispecific antibodies (BsAbs) for pretargeted radioimmunotherapy (PRIT). For optimized delivery of the theranostic γ - and β -emitting isotope ^{177}Lu with DOTA-based PRIT (DOTA-PRIT), bivalent Gemini (DOTA-Bn-thiourea-PEG4-thiourea-Bn-DOTA, aka (3,6,9,12-tetraoxatetradecane-1,14-diyl)bis(DOTA-benzyl thiourea)) was developed. **Methods:** Gemini was synthesized by linking 2 S-2-(4-isothiocyanatobenzyl)-DOTA molecules together via a 1,14-diamino-PEG4 linker. [^{177}Lu]Lu-Gemini was prepared with no-carrier-added $^{177}\text{LuCl}_3$ to a molar-specific activity of 123 GBq/ μmol and radiochemical purity of more than 99%. The specificity of BsAb- ^{177}Lu -Gemini was verified in vitro. Subsequently, we evaluated biodistribution and whole-body clearance for [^{177}Lu]Lu-Gemini and, for comparison, our gold-standard monovalent [^{177}Lu]Lu-S-2-(4-aminobenzyl)-DOTA ([^{177}Lu]Lu-DOTA-Bn) in naïve (tumor-free) athymic nude mice. For our proof-of-concept system, a 3-step pretargeting approach was performed with an established DOTA-PRIT regimen (anti-GPA33/anti-DOTA IgG-scFv BsAb, a clearing agent, and [^{177}Lu]Lu-Gemini) in mouse models. **Results:** Initial in vivo studies showed that [^{177}Lu]Lu-Gemini behaved similarly to [^{177}Lu]Lu-DOTA-Bn, with almost identical blood and whole-body clearance kinetics, as well as biodistribution and mouse kidney dosimetry. Pretargeting [^{177}Lu]Lu-Gemini to GPA33-expressing SW1222 human colorectal xenografts was highly effective, leading to absorbed doses of [^{177}Lu]Lu-Gemini for blood, tumor, liver, spleen, and kidneys of 3.99, 455, 6.93, 5.36, and 14.0 cGy/MBq, respectively. Tumor-to-normal tissue absorbed-dose ratios (i.e., therapeutic indices [TIs]) for the blood and kidneys were 114 and 33, respectively. In addition, we demonstrate that the use of bivalent [^{177}Lu]Lu-Gemini in DOTA-PRIT leads to improved TIs and augmented [^{177}Lu]Lu-Gemini tumor uptake and retention in comparison to monovalent [^{177}Lu]Lu-DOTA-Bn. Finally, we established efficacy in SW1222 tumor-bearing mice, demonstrating that a single injection of anti-GPA33 DOTA-PRIT with 44 MBq (1.2 mCi) of [^{177}Lu]Lu-Gemini (estimated

tumor-absorbed dose, 200 Gy) induced complete responses in 5 of 5 animals and a histologic cure in 2 of 5 (40%) animals. Moreover, a significant increase in survival compared with nontreated controls was noted (maximum tolerated dose not reached). **Conclusion:** We have developed a bivalent DOTA-radiohaptent, [^{177}Lu]Lu-Gemini, that showed improved radiopharmacology for DOTA-PRIT application. The use of bivalent [^{177}Lu]Lu-Gemini in DOTA-PRIT, as opposed to monovalent [^{177}Lu]Lu-DOTA-Bn, allows curative treatments with considerably less administered ^{177}Lu activity while still achieving high TIs for both the blood (>100) and the kidneys (>30).

Key Words: pretargeted radioimmunotherapy; ^{177}Lu ; GPA33; colorectal cancer; multivalent

J Nucl Med 2024; 65:1611–1618

DOI: 10.2967/jnumed.124.267685

Pretargeted radioimmunotherapy (PRIT) seeks to overcome key challenges in effective radiotheranostic treatments (1). These challenges primarily include suboptimal drug delivery and inadequate retention of radionuclides delivered to the target site (2). In dosimetry terms, these properties lead to unfavorable therapeutic indices (TIs) and make curative tumor dosing (3) impossible without dose-limiting normal-tissue toxicity (4).

We are developing a PRIT strategy that combines antitumor/anti-DOTA bispecific antibodies (BsAbs) in either the format of an IgG-svFv (5) or, more recently, a self-assembling disassembling platform (6). These BsAbs contain the single-chain variable fragment antibody C825, which binds the radiometal complex of S-2-(4-aminobenzyl)-DOTA chelate (~10–20 pM for M-DOTA-Bn, where M is yttrium or lutetium) (7). We call this radiotheranostic platform DOTA-based PRIT (DOTA-PRIT). Initially, a nonradioactive BsAb is administered and allowed to accumulate at the tumor. If necessary, a clearing agent is administered to reduce circulating nontumor-bound BsAbs. Lastly, intratumoral C825 efficiently binds low-molecular-weight DOTA-radiohaptent, or it is

Received Feb. 28, 2024; revision accepted Jul. 10, 2024.

For correspondence or reprints, contact Sarah M. Cheal (smc4002@med.cornell.edu).

Published online Aug. 21, 2024.

COPYRIGHT © 2024 by the Society of Nuclear Medicine and Molecular Imaging.

otherwise cleared from the body renally (8). This approach greatly enhances the TIs of conventional radioimmunotherapy by mimicking the radiopharmacology of low- to moderate-molecular-weight radiotheranostics.

We hypothesized that we could implement a multivalent DOTA-radiohaptent to efficiently complex ^{177}Lu and induce cooperative binding by intratumoral C825 while still possessing the optimal radiopharmacologic properties of rapid clearance via a renal route without retention in normal tissue (9). Thus, we can expand the therapeutic window of DOTA-PRIT by combining delayed radiohaptent-tumor complex dissociation with efficient excretion. Modeled after a bivalent radiohaptent for PRIT initially proposed by Gautherot et al. (10) and other established multivalent PRIT approaches, such as janus-DOTA (11), we designed a bivalent DOTA-haptent that we call Gemini (the twin).

Herein, we describe the synthesis and evaluation of Gemini and verified its effectiveness *in vivo* using a model DOTA-PRIT system, anti-GPA33 DOTA-PRIT. We chose GPA33 targeting in colorectal cancer based on our prior clinical experience with a GPA33-targeted antibody (12), high antigen density on most colorectal cancer cells (>95%) (13), and long-term persistence of the antigen-antibody complex on the plasma membrane (14). These properties make the GPA33 antigen target highly appealing for PRIT (1).

MATERIALS AND METHODS

Cell Lines and Animal Models

293T cells expressing huC825 were generated as described previously (15). The GPA33-positive human colorectal cancer cell line SW1222 was obtained from the Ludwig Institute for Cancer Immunotherapy and was maintained in minimal essential medium. 293T cells expressing huC825 was grown in RPMI 1640 medium. All media were obtained from the Memorial Sloan Kettering Cancer Center (MSKCC) Media Core and supplemented with 10% fetal bovine serum, 2 mM L-glutamine, 100 IU/mL penicillin, and 100 $\mu\text{g}/\text{mL}$ streptomycin.

All animal experiments in this study were performed in accordance with protocols approved by the Institutional Animal Care and Use Committee of MSKCC or Weill Cornell Medicine and followed National Institutes of Health guidelines for animal welfare. For all *in vivo* studies, 6- to 8-wk-old female nude mice were used. For DOTA-PRIT, SW1222 tumor-bearing nude mice were used. To establish SW1222 tumors, mice were inoculated with 5.0×10^6 cells in a 200- μL cell suspension of a 1:1 mixture of medium with reconstituted basement membrane (BD Matrigel; Collaborative Biomedical Products) in the lower flank via subcutaneous injection. Palpable tumors (30–300 mm^3) were established within 7–10 d of inoculation.

DOTA-PRIT Reagents

The 3 DOTA-PRIT reagents were anti-GPA33/anti-DOTA IgG-scFv BsAb, a DOTA(Y)-conjugated poly-N-acetyl-galactosamine glycodendron clearing agent, and either bivalent [^{177}Lu]Lu-Gemini (current study) or monovalent [^{177}Lu]Lu-S-2-(4-aminobenzyl)-DOTA ([^{177}Lu]Lu-DOTA-Bn). The BsAb (molecular weight, $\sim 210,000$ g/mol) was produced as previously described (16). The clearing agent (molecular weight, 9,059 g/mol) is designed to rapidly remove the circulating BsAb by forming a complex via the DOTA(Y) moiety and clear via liver asialogalactose receptor recognition and catabolism (17). All reagents were formulated for injection in sterile normal saline up to a 200- μL volume and administered intravenously via the tail vein. The treatment timeline was as follows for all biodistribution and therapy studies: the BsAb was administered at minus 48 h, followed by the

clearing agent at minus 4 h and [^{177}Lu]Lu-Gemini or [^{177}Lu]Lu-DOTA-Bn at 0 h (details of biodistribution and therapy assessment are given later).

Synthesis and Characterization of [^{177}Lu]Lu-Gemini

The Gemini precursor was prepared by reaction of 1,14-diamino-PEG4 and the bifunctional chelator S-2-(4-isothiocyanatobenzyl)-DOTA under basic conditions. The final product was purified using semipreparative reverse-phase C-18 high-pressure liquid chromatography characterized by liquid chromatography-mass spectrometry. [^{177}Lu]LuCl₃ (no carrier added; specific activity, $\sim 3,561$ GBq/mg [623 MBq/nmol]) was obtained from Isotopia. Because only the lanthanide DOTA chelate complex is recognized with high affinity by C825 (7), first ^{177}Lu -radiolabeled Gemini and DOTA-Bn were prepared based on previously described procedures (15), with the addition of $^{\text{nat}}\text{LuCl}_3$ to fill all empty aminobenzyl-DOTA chelation sites. For [^{177}Lu]Lu-Gemini binding assessment, a magnetic bead-based radioligand assay was used (18) and specificity was verified by adding radioligand to BsAb beads containing 5 μg of proteus-DOTA (19). Dissociation assays were performed using 293T cells expressing huC825 (15). More details are provided in the supplemental materials (supplemental materials are available at <http://jnm.snmjournals.org>).

In Vitro Binding and Internalization of BsAb-Pretargeted [^{177}Lu]Lu-Gemini

The kinetics of cellular uptake and retention of [^{177}Lu]Lu-Gemini were evaluated and compared with those of monovalent [^{177}Lu]Lu-DOTA-Bn using previously described methods (20,21). More details are provided in the supplemental materials.

In Vivo Characterization and Dosimetry

Initially, [^{177}Lu]Lu-Gemini or [^{177}Lu]Lu-DOTA-Bn (1.85 MBq [50 μCi], 400 pmol) was administered to groups of naïve (tumor-free) mice ($n = 10$), and a serial biodistribution study was performed in groups of 5 per time point 1 and 3 h after injection. Blood was collected at 5, 30, 60, 120, and 180 min ($n = 5$) and analyzed on a γ -counter, as described later. Whole-body activity was measured at the same time points ($n = 5$) in a CRC-55tR dose calibrator (Capintec). At each biodistribution time point, the mice were anesthetized and killed. The tissues (blood, tumor, heart, liver, spleen, stomach, small intestine, large intestine, kidney, muscle, bone, and tail [site of injection]) were collected and rinsed with phosphate-buffered saline, and the activity in each tissue specimen measured in a Hidex automatic γ -counter. Count rates were background- and decay-corrected, converted to activities using a system calibration factor specific for the isotope, normalized to the administered activity, and expressed as percentage injected activity per gram of tissue (%IA/g).

For DOTA-PRIT biodistribution experiments, groups ($n = 4$ –5/group) of SW1222 tumor-bearing mice were treated with 250 μg (1.19 nmol) of anti-GPA33 BsAb, followed 44 h later with 25 μg (2.76 nmol) of clearing agent. After an additional 4 h, [^{177}Lu]Lu-Gemini (1,850 kBq [50 μCi]/200 pmol) or [^{177}Lu]Lu-DOTA-Bn (1,850 kBq [50 μCi]/400 pmol) was administered. A serial biodistribution study was performed at 2, 24, and 120 h after injection of [^{177}Lu]Lu-Gemini or [^{177}Lu]Lu-DOTA-Bn. Serial biodistribution data were used to calculate dosimetry. More details are provided in the supplemental materials.

Radiopharmaceutical Therapy

For radiopharmaceutical therapy with DOTA-PRIT plus [^{177}Lu]Lu-Gemini, groups ($n = 4$ –5/group) of SW1222 tumor-bearing mice (approximate starting tumor volumes, 33 mm^3) were treated with anti-GPA33 BsAb, clearing agent, and [^{177}Lu]Lu-Gemini (44 MBq [1.2 mCi]/200 pmol) as described earlier. Controls included no treatment and anti-GD2 (22) (nonspecific) pretargeting of [^{177}Lu]Lu-Gemini (i.e., anti-GD2 BsAb in place of anti-GPA33 BsAb). At

24 h after injection of [^{177}Lu]Lu-Gemini, randomly selected mice undergoing treatment were imaged by SPECT/CT using previously described protocols (23) to verify tumor targeting ($n = 3$ or 2 of anti-GPA33 or anti-GD2 pretargeted [^{177}Lu]Lu-Gemini, respectively). Body weights and tumor volumes were measured before the injection and up to twice per week. The tumor volume was determined using an ellipsoid volume formula ($V = 4/3\pi$ (length/2 \times width/2 \times height/2)), with dimensions in millimeters. The study endpoint was 80 d. For hematology, blood was collected from all therapy cohorts via retro-orbital blood draws in tubes containing ethylenediaminetetraacetic acid 18 and 25 d after injection of [^{177}Lu]Lu-Gemini ($n = 4$ –5 mice per time point). Automated analysis was performed on a Drew Scientific HemaVet 950FS (blood parameters analyzed were platelets, white blood cells, neutrophils, red blood cells, lymphocytes, and monocytes). Surviving animals were submitted alive at 80 d to the Laboratory of Comparative Pathology of MSKCC for postmortem pathologic analysis, hematology, and serum chemistry (supplemental materials give anatomic and clinical pathology methods). Immunohistochemical staining of GPA33 on tissues was performed according to previously described methods (16).

Data Analysis

Differences between means were determined using unpaired, 2-tailed Student *t* tests. Differences at the 95% confidence level ($P < 0.05$) were considered statistically significant. All statistical data are reported as mean \pm SD.

RESULTS

Synthesis and in Vitro Characterization of [^{177}Lu]Lu-Gemini

Gemini was prepared in high purity (>98%) and with an overall yield of 78% (Supplemental Fig. 1). Gemini efficiently chelated ^{177}Lu , resulting in average radiochemical conversions of more than 99% with molar activity of 123 GBq/ μmol and radiochemical purity of more than 99% (Fig. 1). Radiochemical purity of [^{177}Lu]Lu-Gemini, as determined by the magnetic bead-based radioligand assay, was $97.7\% \pm 0.10\%$. Based on radiochemical titration of Gemini with no-carrier-added [^{177}Lu]LuCl₃, the apparent specific molar activity is 7.96 GBq/nmol (Supplemental Fig. 2). Thin-layer chromatography analysis detected less than 1% unchelated ^{177}Lu for [^{177}Lu]Lu-Gemini over 7 d in either phosphate-buffered saline or human serum (data not shown). During dissociation assays using 293T cells expressing huC825, we determined a half-life of 12.41 min ($R^2 = 0.9058$) and 7.39 min ($R^2 = 0.9163$) for [^{177}Lu]Lu-Gemini and [^{177}Lu]Lu-DOTA-Bn, respectively ($P < 0.0001$; Supplemental Fig. 3).

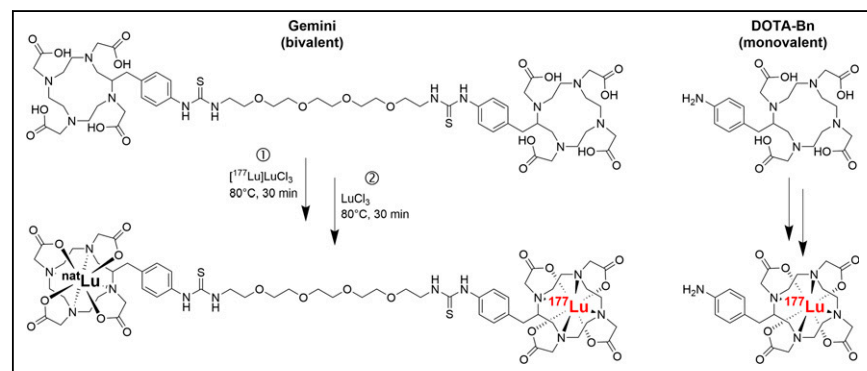


FIGURE 1. Chemical structures of bivalent [^{177}Lu]Lu-Gemini or monovalent [^{177}Lu]Lu-S-2-(4-aminobenzyl)-DOTA ([^{177}Lu]Lu-DOTA-Bn). Radiochemical synthesis of [^{177}Lu]Lu-Gemini (left) and [^{177}Lu]Lu-DOTA-Bn (right) is shown.

Assessment of Anti-GPA33 BsAb-Pretargeted [^{177}Lu]Lu-Gemini Binding and Internalization in GPA33-Positive SW1222 Cells

During the in vitro pretargeting assay with GPA33-positive SW1222 cells, anti-GPA33 BsAb-pretargeted [^{177}Lu]Lu-Gemini rapidly localized to the cell surface and was internalized at 37°C (Fig. 2). A greater proportion of the added tracer [^{177}Lu]Lu-Gemini than of [^{177}Lu]Lu-DOTA-Bn was cell-associated over 24 h (area under the curve [AUC], 616.6 for [^{177}Lu]Lu-DOTA-Bn and 788.9 for [^{177}Lu]Lu-Gemini; $P = 0.0036$; Fig. 2A). Furthermore, [^{177}Lu]Lu-Gemini showed that an increased proportion of cell-associated activity was internalized compared with [^{177}Lu]Lu-DOTA-Bn (AUC, 54.2 [8.8% of cell-associated activity] for [^{177}Lu]Lu-DOTA-Bn and 165.3 [21.0% of cell-associated activity] for [^{177}Lu]Lu-Gemini; $P < 0.0001$; Fig. 2B). The cell-associated fraction of [^{177}Lu]Lu-Gemini or [^{177}Lu]Lu-DOTA-Bn was minimal in the absence of BsAb (<2% at all time points; AUC, 22.5 for [^{177}Lu]Lu-Gemini and 26.1 for [^{177}Lu]Lu-DOTA-Bn), confirming that anti-GPA33 BsAb was required for [^{177}Lu]Lu-Gemini or [^{177}Lu]Lu-DOTA-Bn binding and internalization (Fig. 2A). In summary, in vitro pretargeting with [^{177}Lu]Lu-Gemini versus [^{177}Lu]Lu-DOTA-Bn led to increased cell association (AUC ratio, 1.28) and increased internalization (AUC ratio, 3.05) of ^{177}Lu activity.

In Vivo Characterization of [^{177}Lu]Lu-Gemini in the Absence of BsAb

We performed comparative biodistribution and found the clearance properties of [^{177}Lu]Lu-Gemini and [^{177}Lu]Lu-DOTA-Bn in naïve mice. Summaries of the in vivo properties and mouse kidney dosimetry are provided in Table 1. The data (Supplemental Fig. 4) show little accumulation and retention of the radiotracers in major clearance organs, including the large intestine and kidney.

Serial Biodistribution of DOTA-PRIT and Dosimetry Calculations

During anti-GPA33 DOTA-PRIT plus [^{177}Lu]Lu-Gemini, rapid and efficient SW1222 tumor targeting was observed within 2 h after injection (Fig. 3; Supplemental Table 1). The tumor uptake was 29.50 ± 6.04 %IA/g, which was approximately double that observed during anti-GPA33 DOTA-PRIT plus [^{177}Lu]Lu-DOTA-Bn (16.71 ± 3.04 %IA/g). Furthermore, although the tumor-associated ^{177}Lu activity was observed to rapidly washout for [^{177}Lu]Lu-DOTA-Bn (4.06 ± 0.69 and 1.18 ± 0.16 %IA/g 24 h and 120 h after injection, respectively), the tumor retention of [^{177}Lu]Lu-Gemini significantly improved. At 24 h after injection, the ^{177}Lu activity was essentially unchanged (24.50 ± 12.63 %IA/g), and it decreased by about half to 13.54 ± 3.05 %IA/g 120 h after injection. At 2 h after injection, both blood and kidney uptake were significantly higher for [^{177}Lu]Lu-Gemini than for [^{177}Lu]Lu-DOTA-Bn (blood, 0.41 ± 0.12 vs. 0.16 ± 0.05 %IA/g; $P = 0.00388$; kidney, 1.15 ± 0.14 vs. 0.64 ± 0.09 %IA/g; $P = 0.00038$), but by 120 h, no significant difference was seen for the blood (0.02 ± 0.01 vs. 0.01 ± 0.01 %IA/g; $P = 0.097$). Furthermore, although kidney uptake at 120 h for [^{177}Lu]Lu-Gemini was about 3-fold higher than for [^{177}Lu]Lu-DOTA-Bn

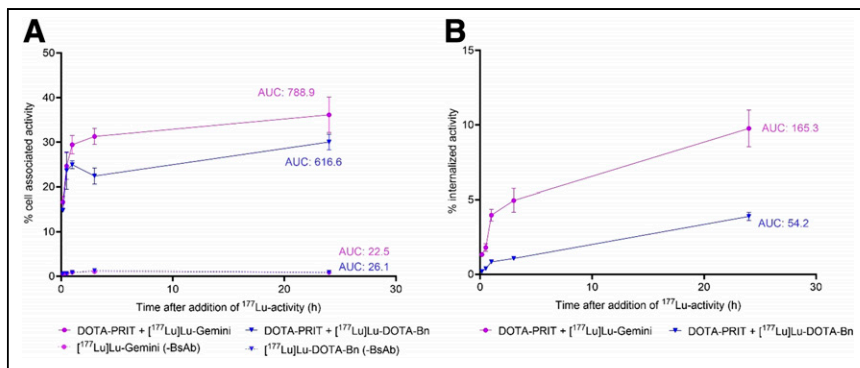


FIGURE 2. In vitro anti-GPA33 DOTA-PRIT + [¹⁷⁷Lu]Lu-Gemini or [¹⁷⁷Lu]Lu-DOTA-Bn in GPA33-positive SW1222 cells up to 24 h after addition of ¹⁷⁷Lu activity. (A) Percentage of cell-associated activity. (B) Percentage of internalized activity. AUC was determined from 10 min to 24 h after addition of ¹⁷⁷Lu activity. Data shown are *n* = 3.

(0.30 ± 0.08 vs. 0.09 ± 0.02 %IA/g; $P = 0.00322$) the uptake was still less than 0.5 %IA/g and thus favorable overall in terms of renal retention of radiolabeled low- to moderate-molecular-weight molecules for targeted radionuclide therapy (24). Dosimetry is provided in Table 2.

Therapy Studies

To establish efficacy with anti-GPA33 DOTA-PRIT plus [¹⁷⁷Lu]Lu-Gemini, single-cycle PRIT was performed in nude mice bearing subcutaneous GPA33-positive SW1222 xenografts. Based on our previous experience with anti-GPA33 DOTA-PRIT plus [¹⁷⁷Lu]Lu-DOTA-Bn in the same mouse model, a high probability of a histologically verified cure can be achieved with a cumulative tumor-absorbed dose of 100 Gy given over 3 treatment cycles (23). To achieve a potentially curative dose of 100 Gy to SW1222 tumor, the administered activity required is 143 or 23 MBq (6-fold less) of [¹⁷⁷Lu]Lu-DOTA-Bn or [¹⁷⁷Lu]Lu-Gemini, respectively (Table 2). Therefore, in consideration that a single-cycle treatment is planned here instead a 3-cycle regimen, we hypothesized that anti-GPA33 DOTA-PRIT plus 44.4 MBq of [¹⁷⁷Lu]Lu-Gemini would be safe, as well as highly effective. At this activity level, the estimated absorbed dose delivered to the tumor would be 20,202 cGy (202 Gy), with 177 cGy delivered to the blood (marrow) and 622 cGy delivered to the kidney.

The therapy results are summarized in Figures 4A and 4B and Supplemental Figures 5 and 6. SW1222 tumor-bearing mice treated with anti-GPA33 DOTA-PRIT plus 44.4 MBq of [¹⁷⁷Lu]Lu-Gemini showed significantly enhanced survival over nontreated controls and nontargeted controls (log-rank, $P < 0.0001$). The median survival was 24.5 d, 39 d, and not yet reached (>80 d) for nontreated, anti-GD2 (nonspecific) DOTA-PRIT plus 44.4 MBq

of [¹⁷⁷Lu]Lu-Gemini, and anti-GPA33 DOTA-PRIT plus 44.4 MBq of [¹⁷⁷Lu]Lu-Gemini mice, respectively. Complete responses (defined as tumor regression to below the measurable ellipsoidal tumor volume [<4.2 mm³] using manual calipers) were observed in 5 of 5 (100%) GPA33-treated mice and 1 of 5 (20%) GD2-treated mice. By 80 d, tumors from 2 of 5 GPA33-treated mice and the single GD2-treated mouse with a complete response had recurred. Of the 5 GPA33-treated surviving mice, 2 of them had no detectable neoplasia in the skin and underlying connective tissues. The site of tumor implantation in these cases was composed of a fibrocollagenous matrix containing fibroblasts and stromal spindle

cells (Supplemental Fig. 7). Residual tumors present in the remaining 3 GPA33-treated and GD2-treated mice were consistent with an adenocarcinoma (Supplemental Fig. 7) and GPA33 expression was observed by immunohistochemistry (Supplemental Fig. 8), suggesting that retreatment with anti-GPA33 DOTA-PRIT is feasible.

As shown in Figure 5, SPECT/CT images obtained from randomly selected mice undergoing treatment with anti-GPA33 DOTA-PRIT plus 44.4 MBq of [¹⁷⁷Lu]Lu-Gemini revealed highly efficient tumor targeting (average tumor uptake, 16.8 %IA/cm³; tumor-to-normal tissue uptake ratios, 32.9, 20.2, and 58.3, for heart, kidney, and bone, respectively). Although negligible tumor targeting was observed in mice treated with control anti-GD2 DOTA-PRIT plus 44.4 MBq of [¹⁷⁷Lu]Lu-Gemini (average tumor uptake, 1.9 %IA/cc), enhanced blood-pool activity was evident, corresponding to a tumor-to-normal tissue uptake ratio of 0.4 for the heart. In addition, for this control treatment, unfavorable tumor-to-normal tissue uptake ratios of 1.5 for the kidney and 1.4 for bone were observed.

Toxicity

All treatments were well tolerated. No treatment groups showed average weight loss greater than 15% of pretreatment baseline (Supplemental Fig. 6). Hematologic (respective concentrations of white blood cells, platelets, and neutrophils $\times 10^3/\mu\text{L}$) analysis at 18 d after treatment initiation revealed myelosuppression in anti-GD2 (nonspecific) DOTA-PRIT plus 44.4 MBq of [¹⁷⁷Lu]Lu-Gemini (1.13 ± 0.58 , 458 ± 327 , and 0.62 ± 0.31 , respectively) versus the pretreatment baseline (5.54 ± 1.83 , $1,031 \pm 134$, and 1.69 ± 0.42 , respectively) and anti-GPA33 DOTA-PRIT plus

TABLE 1
In Vivo Characterization of [¹⁷⁷Lu]Lu-Gemini and Calculated Mouse Dosimetry for Kidney, Blood, and Bone Marrow

DOTA-radiohaptent	Blood half-life (min)	Whole-body half-life (min)	Kidney uptake 3 h after injection (%IA/g)	Kidney dosimetry (mGy/MBq)	Blood dosimetry (mGy/MBq)	Bone marrow dosimetry (mGy/MBq)
[¹⁷⁷ Lu]Lu-Gemini	10.12	29.06	0.57 ± 0.29	100.88	0.97	0.35
[¹⁷⁷ Lu]Lu-DOTA-Bn	11.94	27.46	0.59 ± 0.45	104.78	1.06	0.38

For comparison, [¹⁷⁷Lu]Lu-DOTA-Bn was investigated using the identical protocol.

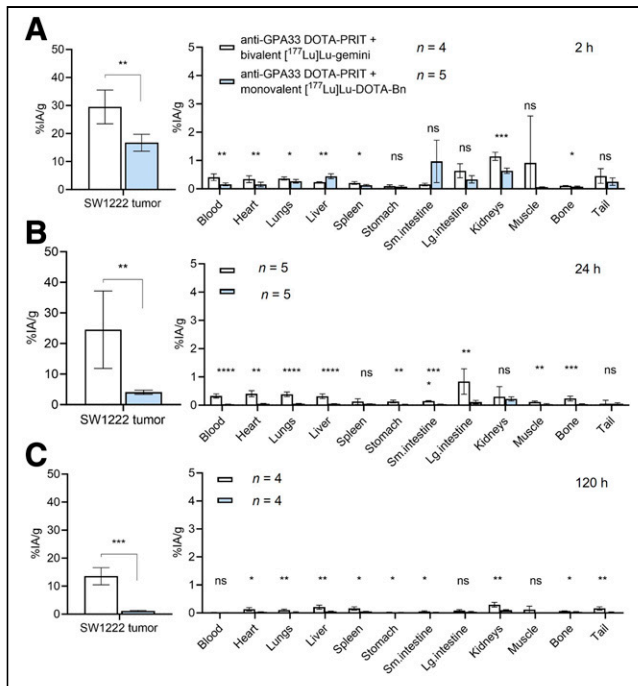


FIGURE 3. Anti-GPA33 DOTA-PRIT serial biodistribution data in mouse model of human colorectal cancer. (A–C) Ex vivo biodistribution assay at 2 h (A), 24 h (B), or 120 h (C) after administration of GPA33-pretargeted [¹⁷⁷Lu]Lu-Gemini (~1,850 kBq [50 μCi]/200 pmol) or [¹⁷⁷Lu]Lu-DOTA-Bn (~1,850 kBq [50 μCi]/400 pmol) into groups of nude mice bearing subcutaneous SW1222 xenografts (*n* = 4–5/group). **P* < 0.05. ***P* < 0.01. ****P* < 0.001. *****P* < 0.0001. Lg. = large; ns = no significant difference; Sm = small.

44.4 MBq of [¹⁷⁷Lu]Lu-Gemini (5.58 ± 1.60, 861 ± 120, and 1.69 ± 0.31, respectively). No significant differences were observed in concentrations of white blood cells, platelets, or neutrophils between anti-GPA33 DOTA-PRIT plus 44.4 MBq of [¹⁷⁷Lu]Lu-Gemini treatment and no treatment control.

Additional hematology data are provided in Supplemental Table 2.

Seven survivors (2 treated with anti-GD2 [nonspecific] DOTA-PRIT plus 44.4 MBq of [¹⁷⁷Lu]Lu-Gemini and 5 treated with anti-GPA33 DOTA-PRIT plus 44.4 MBq of [¹⁷⁷Lu]Lu-Gemini) were submitted for complete necropsy (Supplemental Table 3), complete blood count with automated differential (Supplemental Table 4), and complete metabolic panel (Supplemental Table 5) at 80 d. Histopathology of the kidney, bone marrow, and ovary from representative mice treated with either anti-GPA33 DOTA-PRIT plus [¹⁷⁷Lu]Lu-Gemini or anti-GD2 (nonspecific) DOTA-PRIT plus [¹⁷⁷Lu]Lu-Gemini is shown in Figure 6. The ovaries were small with atrophied cortices and partial to complete absence of developing follicles, oocytes, or corpora luteum (Fig. 6). The ovarian atrophy seen in these mice is an unusual finding for the age and the mouse strain used in this study. We have previously observed this lesion in ovaries in nude mice used in radioimmunotherapy studies using ¹⁷⁷Lu (6,25). In these cases, ovarian atrophy is compatible with radiation-induced toxicity to germ cells, which may represent an off-target effect of the treatment to this organ (e.g., cross-fire effect from adjacent organs such as the kidneys or bladder). There were no microscopic changes compatible with toxicity in the kidneys, urinary bladder, liver, spleen, and bone marrow, which are

TABLE 2
Absorbed Doses for Anti-GPA33 DOTA-PRIT with [¹⁷⁷Lu]Lu-Gemini or [¹⁷⁷Lu]Lu-DOTA-Bn in Nude Mice Bearing Subcutaneous SW1222 Xenografts

Tissue	[¹⁷⁷ Lu]Lu-Gemini		[¹⁷⁷ Lu]Lu-DOTA-Bn	
	Absorbed dose (cGy/MBq)	TI	Absorbed dose (cGy/MBq)	TI
Blood	3.99	114	0.50	140
SW1222 tumor	455	—	69.79	—
Heart	2.62	174	1.45	48
Lungs	5.16	88	2.55	27
Liver	6.93	66	2.16	32
Spleen	5.36	85	1.86	38
Stomach	0.61	746	0.27	258
Small intestine	1.13	403	0.73	96
Large intestine	1.44	316	0.91	77
Kidneys	14.0	33	3.94	18
Muscle	3.84	118	0.43	162
Bone	2.09	218	1.26	55

tissues that could be affected by radiotoxicity induced by different ¹⁷⁷Lu radioimmunotherapy modalities (26,27). Additional microscopic findings are presented in Supplemental Table 3 and were considered incidental findings or spontaneous background changes commonly seen laboratory mouse strains (28).

The complete blood cell counts showed no significant differences among groups or deviation from reference ranges

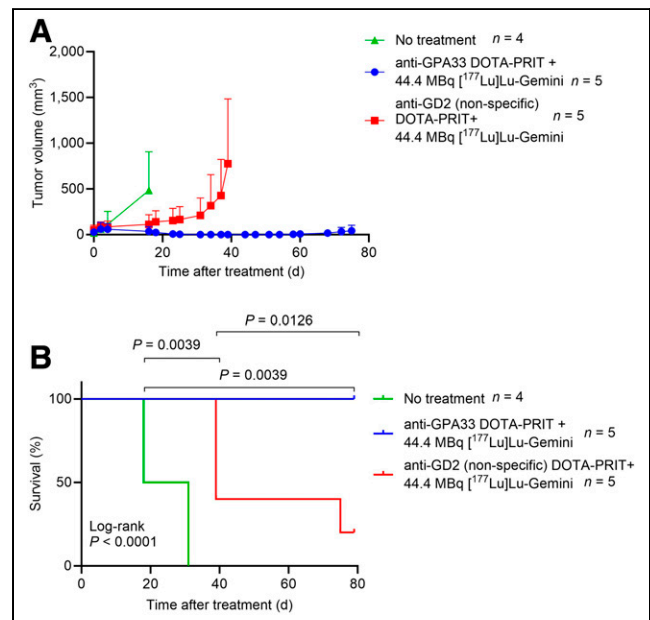


FIGURE 4. Efficacy and toxicity of DOTA-PRIT + [¹⁷⁷Lu]Lu-Gemini in SW1222 tumor-bearing mice. Tumor-bearing mice were given single injection of anti-GPA33 DOTA-PRIT + [¹⁷⁷Lu]Lu-Gemini (44.4 MBq [1.2 mCi], 200 pmol) or anti-GD2 (nonspecific) DOTA-PRIT + [¹⁷⁷Lu]Lu-Gemini (44.4 MBq [1.2 mCi], 200 pmol). (A) Tumor response. (B) Kaplan-Meier survival.

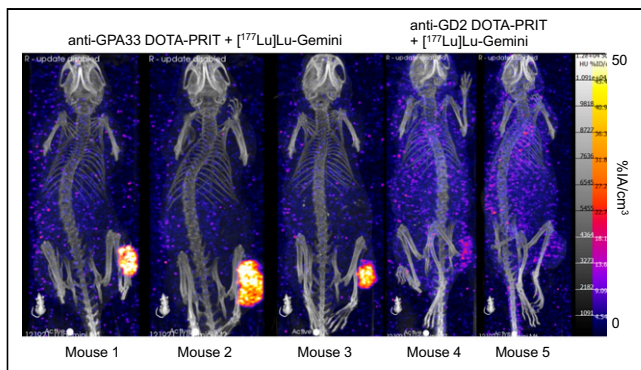


FIGURE 5. SPECT/CT images obtained from randomly selected mice undergoing DOTA-PRIT + $[^{177}\text{Lu}]\text{Lu-Gemini}$ (44.4 MBq [1.2 mCi], 200 pmol) 24 h after administration of $[^{177}\text{Lu}]\text{Lu-Gemini}$. Shown is $n = 3$ from anti-GPA33 DOTA-PRIT + 44.4 MBq of $[^{177}\text{Lu}]\text{Lu-Gemini}$ (mouse 1 to mouse 3) and $n = 2$ from anti-GD2 (nonspecific) DOTA-PRIT + 44.4 MBq of $[^{177}\text{Lu}]\text{Lu-Gemini}$ (mouse 4 and mouse 5).

(Supplemental Table 4). On serum chemistry (Supplemental Table 4), 3 of 5 anti-GPA33 DOTA-PRIT plus $[^{177}\text{Lu}]\text{Lu-Gemini}$ mice and all (2/2) anti-GD2 (nonspecific) DOTA-PRIT plus $[^{177}\text{Lu}]\text{Lu-Gemini}$ mice have a mild to moderate increase in aspartate aminotransferase. The average blood urea nitrogen and creatinine levels in the GPA33-treated (5/5) and GD2-treated (2/2) mice were normal, indicating adequate renal function after radiation treatment.

DISCUSSION

We have successfully identified a bivalent DOTA-radiohapten for DOTA-PRIT that leads to highly favorable TIs for key organs at risk, with enhanced uptake and retention in tumors in relationship to the blood (a surrogate for marrow) and the kidney. In vitro studies revealed that anti-GPA33 DOTA-PRIT plus $[^{177}\text{Lu}]\text{Lu-Gemini}$ led to increased cellular retention of ^{177}Lu activity (Fig. 2) and exhibited slower dissociation kinetics (Supplemental Fig. 3) than did anti-GPA33 DOTA-PRIT plus $[^{177}\text{Lu}]\text{Lu-DOTA-Bn}$. Further analysis is needed to understand the underlying mechanism, and planned future studies will explore the structure–function relationships related to these improved tumor retention properties.

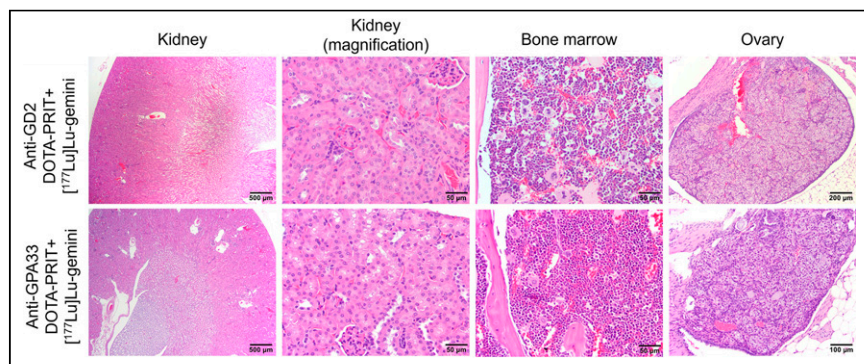


FIGURE 6. Necropsy and histopathology were performed in surviving animals at 80 d. Representative mice treated with either anti-GPA33 DOTA-PRIT + $[^{177}\text{Lu}]\text{Lu-Gemini}$ or anti-GD2 (nonspecific) DOTA-PRIT + $[^{177}\text{Lu}]\text{Lu-Gemini}$ are shown. Representative sections of kidney, bone marrow (femur), and abnormal ovary are shown. Ovarian cortices in both mice were diffusely atrophied with complete absence of follicular structures and corpus luteus.

Multivalent radiopharmaceuticals can increase absolute uptake, prolong apparent dissociation half-time, and show significant increases in internalization rate compared with monovalent controls (29). Current DOTA-PRIT regimens use a monovalent DOTA-hapten as a radiocARRIER (1). Other groups developing PRIT have examined the effects of radiohapten valency on tumor uptake, showing that enhancements to TI are feasible (1).

We previously showed that a 3-cycle regimen of anti-GPA33 DOTA-PRIT plus 55.5 MBq of $[^{177}\text{Lu}]\text{Lu-DOTA-Bn}$ led to a high probability of cure without toxicity in nude mice bearing subcutaneous SW1222 tumors (23). However, we reasoned that substitution of $[^{177}\text{Lu}]\text{Lu-DOTA-Bn}$ with $[^{177}\text{Lu}]\text{Lu-Gemini}$ could lead to greater tumor-absorbed doses without compromise of TIs. By combining anti-GPA33 DOTA-PRIT with $[^{177}\text{Lu}]\text{Lu-Gemini}$, we observed an increased SW1222 tumor-absorbed dose ($\sim 70\text{--}455\text{ cGy/MBq}$ for $[^{177}\text{Lu}]\text{Lu-DOTA-Bn}$ or $[^{177}\text{Lu}]\text{Lu-Gemini}$) while maintaining high TIs to the blood (113) and kidneys (33). In the current study, treatment of subcutaneous SW1222 tumor-bearing mice with a single-injection regimen of anti-GPA33 DOTA-PRIT with 44.4 MBq of $[^{177}\text{Lu}]\text{Lu-Gemini}$ led to 5 of 5 (100%) complete responses and a histologic cure in 2 of 5 (40%) animals. Given that 100% histologic cure was not achieved and serious toxicity was not observed, it is essential to refine the current treatment regimen to strike balance between efficacy and toxicity.

GPA33 expression has been documented in various solid tumors, including in more than 95% of primary and metastatic colorectal cancers and in 50% of gastric and pancreatic cancers (30,31). We have shown the efficacy of this general methodology using anti-GPA33 DOTA-PRIT but intend to explore the hypothesis that enhanced benefits of efficacy will be provided by the multivalency of $[^{177}\text{Lu}]\text{Lu-Gemini}$ in these diverse tumor types and clinical states. In addition, DOTA-PRIT is a versatile platform applicable to a range of tumor antigens (1). Future studies will explore the potential advantages of multivalency for additional antigen–antigen pairs and different tumor states, considering varying antigen densities.

Application of $[^{177}\text{Lu}]\text{Lu-Gemini}$ to DOTA-PRIT led to a dramatic reduction in the administered activity necessary to achieve a histologic cure in the current subcutaneous SW1222 tumor-bearing animal model, which will potentially translate to cost savings and less radiation hazard to patients and treatment staff. Despite this success, and although no toxicity was observed, we acknowledge that the absorbed dose for the blood was increased with $[^{177}\text{Lu}]\text{Lu-Gemini}$ ($\sim 8\text{-fold}$ compared with $[^{177}\text{Lu}]\text{Lu-DOTA-Bn}$). In some clinical situations, this could have consequences, limiting maximum achievable tumor doses. Therefore, using the current 3-step anti-GPA33 DOTA-PRIT regimen, further improvement of the clearing agent can potentially minimize the trade-off between tumor and red marrow radiation-absorbed doses.

CONCLUSION

By using $[^{177}\text{Lu}]\text{Lu-Gemini}$ during anti-GPA33 DOTA-PRIT, we have improved the delivered tumor radiation-absorbed

dose per unit of administered radioactivity (cGy/MBq) while maintaining high TIs to the blood (>100) and kidneys (>30). This will translate to less radiation hazard to patients and hospital staff and significantly reduce radioisotope costs during manufacture.

DISCLOSURE

This research was funded in part by the Hedvig Hricak Chair in Radiology (to Steven Larson), Enid A. Haupt Chair (to Nai Kong Cheung), Center for Targeted Radioimmunotherapy and Theranostics, Ludwig Center for Cancer Immunotherapy of MSKCC (to Steven Larson), and Mr. William H. Goodwin and Mrs. Alice Goodwin and the Commonwealth Foundation for Cancer Research and the Experimental Therapeutics Center of MSKCC (to Steven Larson). Steven Larson was also supported in part by P50-CA86438. This study also received support from R01-CA233896 (to Sarah Cheal). We also acknowledge P30-CA008748 for use of the Tri-Institutional Laboratory of Comparative Pathology of MSKCC, Weill Cornell Medicine, and Rockefeller University; technical services provided by the MSKCC Small-Animal Imaging Core Facility and Laboratory of Comparative Pathology; and the Molecular Cytology Core Facility. Funding for the Organic Synthesis Core is provided through the NCI core grant P30 CA008748 and by NCI R50 CA243895-01 (to Ouathék Ouerfelli). Both MSKCC and Nai Kong Cheung have financial interest in Y-mAbs Therapeutics, Inc.; Abpro-Labs; and Lallemand-Biotec Pharmacon. Nai Kong Cheung reports receiving commercial research grants from Y-mAbs Therapeutics, Inc., and Abpro-Labs. Nai Kong Cheung was named as inventor on multiple patents filed by MSKCC, including those licensed to Y-mAbs Therapeutics, Inc.; Lallemand-Biotec Pharmacon; and Abpro-Labs. Nai Kong Cheung is a scientific advisory board member for Eureka Therapeutics. Nai Kong Cheung, Steven Larson, and Sarah Cheal were named as inventors in the following patent applications relating to GPA33: SK2014-074, SK2015-091, SK2017-079, SK2018-045, SK2014-116, SK2016-052, and SK2018-068 filed by MSKCC. Steven Larson reports receiving commercial research grants from Genentech, Inc.; Willex AG; Telix Pharmaceuticals Ltd.; and Regeneron Pharmaceuticals, Inc.; holding ownership interest or equity in Elucida Oncology, Inc., and Y-mAbs Therapeutics, Inc.; and holding stock in ImaginAb, Inc. Steven Larson is the inventor and owner of issued patents, both unlicensed and licensed, by MSKCC to Samus Therapeutics, Inc.; Elucida Oncology, Inc.; and Y-mAbs Therapeutics, Inc. Steven Larson serves or has served as a consultant to Y-mAbs Therapeutics, Inc.; Cynvec; Eli Lilly & Co.; Prescient Therapeutics Ltd.; Advanced Innovative Partners; Gerson Lehrman Group; Progenics Pharmaceuticals, Inc.; and Janssen Pharmaceuticals, Inc. Steven Larson also acknowledges consultation for Medimagetric LLC and is a Special Government Employee to National Cancer Institute, Molecular Imaging Laboratory, Peter Choyke, Branch Chief. Guangbin Yang and Ouathék Ouerfelli are listed as inventors and receive royalties from patents that were filed by MSKCC. Ouathék Ouerfelli is an unpaid member of the scientific advisory board of Angiogenex and owns shares in Angiogenex. Simone Krebs is supported in part by NIH R37 CA262557, Mr. William H. Goodwin and Mrs. Alice Goodwin and the Commonwealth Foundation for Cancer Research and The Center for Experimental Therapeutics of MSKCC, and flexTDF Award. Simone Krebs has consulted for Telix Pharmaceuticals Ltd. and acknowledges support for

investigator services from RayzeBio. Simone Krebs, Steven Larson, Nai Kong Cheung, Ouathék Ouerfelli, Guangbin Yang, Darren Veach, and Sarah Cheal were named as inventors in PCT/US2021/039418 (tumor homing radio-emitting cell). No other potential conflict of interest relevant to this article was reported.

KEY POINTS

QUESTION: Can a bivalent DOTA-radiohapten be applied to DOTA-PRIT to significantly improve the delivered tumor radiation-absorbed dose?

PERTINENT FINDINGS: We identified a bivalent DOTA-radiohapten for ^{177}Lu (^{177}Lu Lu-Gemini) with pharmacokinetic and biodistribution properties similar to those of the gold-standard monovalent DOTA-hapten [^{177}Lu]Lu-DOTA-Bn. Delivery of [^{177}Lu]Lu-Gemini to subcutaneous GPA33-expressing SW1222 xenografts using a GPA33-DOTA-PRIT approach was highly efficient, leading to an approximately 6.5-fold increase in the tumor radiation-absorbed dose. TIs were also improved, apart from that of the blood (140 vs. 114 for [^{177}Lu]Lu-DOTA-Bn vs. [^{177}Lu]Lu-Gemini). Using a single treatment cycle, complete responses (5/5, 100%) and a histologic cure (2/5, 40%) were achieved without treatment-related toxicities.

IMPLICATIONS FOR PATIENT CARE: GPA33-DOTA-PRIT plus [^{177}Lu]Lu-Gemini allows tumoricidal therapy with significantly reduced administered activity compared with first-generation GPA33-DOTA-PRIT plus [^{177}Lu]Lu-DOTA-Bn. This offers significant safety and logistical benefits for both patients and staff.

REFERENCES

- Cheal SM, Chung SK, Vaughn BA, Cheung N-KV, Larson SM. Pretargeting: a path forward for radioimmunotherapy. *J Nucl Med.* 2022;63:1302–1315.
- Bodei L, Herrmann K, Schoder H, Scott AM, Lewis JS. Radiotheranostics in oncology: current challenges and emerging opportunities. *Nat Rev Clin Oncol.* 2022;19:534–550.
- Sgouros G, Dewaraja YK, Escorcía F, et al. Tumor response to radiopharmaceutical therapies: the knowns and the unknowns. *J Nucl Med.* 2021;62:12S–22S.
- Wahl RL, Sgouros G, Irvani A, et al. Normal-tissue tolerance to radiopharmaceutical therapies, the knowns and the unknowns. *J Nucl Med.* 2021;62:23S–35S.
- Orcutt KD, Ackerman ME, Cieslewicz M, et al. A modular IgG-scFv bispecific antibody topology. *Protein Eng Des Sel.* 2010;23:221–228.
- Santich BH, Cheal SM, Ahmed M, et al. A self-assembling and disassembling (SADA) bispecific antibody (BsAb) platform for curative two-step pretargeted radioimmunotherapy. *Clin Cancer Res.* 2021;27:532–541.
- Orcutt KD, Slusarczyk AL, Cieslewicz M, et al. Engineering an antibody with picomolar affinity to DOTA chelates of multiple radionuclides for pretargeted radioimmunotherapy and imaging. *Nucl Med Biol.* 2011;38:223–233.
- Orcutt KD, Rhoden JJ, Ruiz-Yi B, Frangioni JV, Wittrup KD. Effect of small-molecule-binding affinity on tumor uptake in vivo: a systematic study using a pretargeted bispecific antibody. *Mol Cancer Ther.* 2012;11:1365–1372.
- Orcutt KD, Nasr KA, Whitehead DG, Frangioni JV, Wittrup KD. Biodistribution and clearance of small molecule hapten chelates for pretargeted radioimmunotherapy. *Mol Imaging Biol.* 2011;13:215–221.
- Gautherot E, Le Doussal JM, Bouhou J, et al. Delivery of therapeutic doses of radioiodine using bispecific antibody-targeted bivalent haptens. *J Nucl Med.* 1998;39:1937–1943.
- Goodwin DA, Meares CF, Watanabe N, et al. Pharmacokinetics of pretargeted monoclonal antibody 2D12.5 and ^{88}Y -janus-2-(*p*-nitrobenzyl)-1,4,7,10-tetraazacyclododecanetetraacetic acid (DOTA) in BALB/c mice with KHJ mouse adenocarcinoma: a model for ^{90}Y radioimmunotherapy. *Cancer Res.* 1994;54:5937–5946.
- O'Donoghue JA, Smith-Jones PM, Humm JL, et al. ^{124}I -huA33 antibody uptake is driven by A33 antigen concentration in tissues from colorectal cancer patients imaged by immuno-PET. *J Nucl Med.* 2011;52:1878–1885.

13. Garinchesa P, Sakamoto J, Welt S, Real F, Rettig W, Old L. Organ-specific expression of the colon cancer antigen A33, a cell surface target for antibody-based therapy. *Int J Oncol*. 1996;9:465–471.
14. Ackerman ME, Chalouni C, Schmidt MM, et al. A33 antigen displays persistent surface expression. *Cancer Immunol Immunother*. 2008;57:1017–1027.
15. Dacek MM, Veach DR, Cheal SM, et al. Engineered cells as a test platform for radiohaptens in pretargeted imaging and radioimmunotherapy applications. *Bioconjug Chem*. 2021;32:649–654.
16. Cheal SM, Xu H, Guo HF, et al. Theranostic pretargeted radioimmunotherapy of colorectal cancer xenografts in mice using picomolar affinity ⁸⁶Y- or ¹⁷⁷Lu-DOTA-Bn binding scFv C825/GPA33 IgG bispecific immunoconjugates. *Eur J Nucl Med Mol Imaging*. 2016;43:925–937.
17. Cheal SM, Patel M, Yang G, et al. An N-acetylgalactosamine dendron-clearing agent for high-therapeutic-index DOTA-hapten pretargeted radioimmunotherapy. *Bioconjug Chem*. 2020;31:501–506.
18. Sharma SK, Lyashchenko SK, Park HA, et al. A rapid bead-based radioligand binding assay for the determination of target-binding fraction and quality control of radiopharmaceuticals. *Nucl Med Biol*. 2019;71:32–38.
19. Chung SK, Vargas DB, Chandler CS, et al. Efficacy of HER2-targeted intraperitoneal ²²⁵Ac α-pretargeted radioimmunotherapy for small-volume ovarian peritoneal carcinomatosis. *J Nucl Med*. 2023;64:1439–1445.
20. Heskamp S, Hernandez R, Molkenboer-Kuene JDM, et al. α- versus β-emitting radionuclides for pretargeted radioimmunotherapy of carcinoembryonic antigen-expressing human colon cancer xenografts. *J Nucl Med*. 2017;58:926–933.
21. Chung SK, Vargas DB, Chandler CS, et al. Efficacy of HER2-targeted intraperitoneal ²²⁵Ac α-pretargeted radioimmunotherapy for small-volume ovarian peritoneal carcinomatosis. *J Nucl Med*. 2023;64:1439–1445.
22. Cheal SM, Xu H, Guo HF, Zanzonico PB, Larson SM, Cheung NK. Preclinical evaluation of multistep targeting of diasialoganglioside GD2 using an IgG-scFv bispecific antibody with high affinity for GD2 and DOTA metal complex. *Mol Cancer Ther*. 2014;13:1803–1812.
23. Cheal SM, Fung EK, Patel M, et al. Curative multicycle radioimmunotherapy monitored by quantitative SPECT/CT-based theranostics, using bispecific antibody pretargeting strategy in colorectal cancer. *J Nucl Med*. 2017;58:1735–1742.
24. de Roode KE, Joosten L, Behe M. Towards the magic radioactive bullet: improving targeted radionuclide therapy by reducing the renal retention of radioligands. *Pharmaceuticals (Basel)*. 2024;17:256.
25. Chandler CS, Bell MM, Chung SK, et al. Intraperitoneal pretargeted radioimmunotherapy for colorectal peritoneal carcinomatosis. *Mol Cancer Ther*. 2022;21:125–137.
26. Repetto-Llamazares AH, Larsen RH, Giusti AM, et al. ¹⁷⁷Lu-DOTA-HH1, a novel anti-CD37 radio-immunoconjugate: a study of toxicity in nude mice. *PLoS One*. 2014;9:e103070.
27. Kristiansson A, Ahlstedt J, Holmqvist B, et al. Protection of kidney function with human antioxidation protein α₁-microglobulin in a mouse ¹⁷⁷Lu-DOTATATE radiation therapy model. *Antioxid Redox Signal*. 2019;30:1746–1759.
28. McInnes EF, Mann P. *Background Lesions in Laboratory Animals: A Color Atlas*. Saunders; 2012:45–71.
29. Carlucci G, Ananias HJ, Yu Z, et al. Multimerization improves targeting of peptide radio-pharmaceuticals. *Curr Pharm Des*. 2012;18:2501–2516.
30. Carrasquillo JA, Pandit-Taskar N, O'Donoghue JA, et al. ¹²⁴I-huA33 antibody PET of colorectal cancer. *J Nucl Med*. 2011;52:1173–1180.
31. Sakamoto J, Kojima H, Kato J, Hamashima H, Suzuki H. Organ-specific expression of the intestinal epithelium-related antigen A33, a cell surface target for antibody-based imaging and treatment in gastrointestinal cancer. *Cancer Chemother Pharmacol*. 2000;46(suppl):S27–S32.